Digest Journal of Nanomaterials and Biostructures Vol. 6, No 4, October - December 2011, p. 1859-1865

EUROPIUM CONCENTRATION EFFECT OF EUROPIUM DOPED HYDROXYAPATITE ON PROLIFERATION OF OSTEOBLAST CELLS

F. FRUMOSU, S.L. ICONARU, D. PREDOI*
National Institute for Physics of Materials, P.O. Box MG 07, Bucharest, Magurele, Romania

The aim of this paper is the preparation and characterization of hydroxyapatite doped with europium (Eu^{3+}, Eu:Hap).The nanopowders were obtained by coprecipitation method and analyzed through infrared spectroscopy (FT-IR) and Fourier transform Raman spectroscopy (FT-Raman). The preliminary results reveal the nanometric dimension of the particles and indicate that Eu^{3+} has been introduced into the framework of HAp. The Eu concentration effects of nano Eu:HAp were studied on human osteoblast MG 63 cells in vitro. Our results demonstrate that cell proliferation is not related to the Eu concentration in the HAp particles. This work provides an interesting view of the role of nano Eu:HAp as ideal biomedical materials in future clinical applications.

(Received November 29, 2011; accepted December 5, 2011)

Keywords: Hydroxyapatite, Nanoparticles, Europium, Cell proliferation

1. Introduction

The first structural identifications of biominerals using X-ray diffraction were obtained by de Jong in 1926 [1]. He established that calcium phosphate biominerals of vertebrates corresponded to an apatite structure and since that time bone mineral has been frequently identified as hydroxyapatite (HAp): $Ca_{10}(PO_4)_6(OH)_2$ which was later considered to crystallize in the hexagonal system (space group P63/m).

HAp is also being processed for other biomaterials uses such as the coating of metallic prostheses where it was found to considerably improve bone repair as an "osteoconductive" material or composite ceramic-polymer materials showing strong mechanical analogies with bone tissues and excellent bone bonding abilities [2-3]. In the non-stoichiometric form, ion-substituted and calcium-deficient hydroxyapatite (commonly referred to as ‘‘biological apatite’’), calcium orthophosphates are present in bones, teeth, tendons of mammals, giving these organs stability, hardness and function [4-5].

Synthetic apatites can be prepared by several methods (precipitation under conditions of constant or changing composition, hydrolysis, solid/solid reaction at high temperature, hydrothermal methods) the type of which determines the amount and kind of substitution in the apatite [6-7].

Several processes (precipitation by double decomposition, sol-gel method, hydrolysis) involving various media (aqueous, hydro-alcoholic or organic solutions) leading to calcium phosphate apatites have been also reported [8-11]. Apatite-type compounds are known to exhibit good luminescence characteristics [12-21]. Europium is a well-known and thoroughly investigated active element in the field of lighting and display [17]. Luminescent properties of europium depend strongly on the crystal structure of the host materials.

HAp crystals have been widely used in delivery systems for genes [18], proteins [19] and various drugs [20-21] due to their non-toxicity and excellent biocompatibility, as have been experimentally proven by recent reports [22-25].

* Corresponding author: dpredoi@gmail.com

Photo-induced luminescence is very powerful and useful in situ investigations [26]. Labeling using organic fluorescent molecules is popular in clinical use for years. In recent years, a lot of inorganic components even nanoparticles were suggested to be such candidates. The toxicity of particles used is extremely an important tissue in practical application due to composition and size of nanoparticle. Europium is a luminescent agent with great bio-compatibility and is ideal for implantation and clinical application.

In this study, europium doped hydroxyapatite with an atomic ratio Eu/(Eu +Ca) between 0.5% and 1.5% were synthesized by co-precipitation. The vibrational properties were studied by Fourier transform infrared spectroscopy (FT-IR) and Fourier transforms Raman spectroscopy (FT-Raman).

2. Experimental

2.1 Sample preparation

Hydroxyapatite doped with europium was prepared following the method already described [27]. All the reagents for synthesis including ammonium dihydrogen phosphate [$(NH_4)_2HPO_4$], calcium nitrate [$Ca(NO_3)_2{\cdot}4H_2O$], and europium nitrate [$Eu(NO_3)_3{\cdot}5H_2O$] (Sigma Aldrich) were purchased without further purification. Europium-doped hydroxyapatite was obtained at 80^0C. The powder was obtained by mixing $Eu(NO_3)_3{\cdot}6H_2O$, $Ca(NO_3)_2{\cdot}4H_2O$ and $(NH_4)_2HPO_4$ in deionizated water together (with Ca/P molar ratio: 1.67 and atomic ratio Eu/(Eu +Ca)=0.5% and 1.5%, respectively) and stirred until a homogeneous solution was formed. The obtained precipitate was then filtered, washed several times with deionizated water. The resulting material was dried at 80 ^{0}C for 72h.

2.2 Sample characterization

Transmission Electron Microscopy (TEM) studies were carried out using a JEOL 200 CX. The specimen for TEM imaging was prepared from the particles suspension in deionized water. A drop of well-dispersed supernatant was placed on a carbon – coated 200 mesh copper grid, followed by drying the sample at ambient conditions before it is attached to the sample holder on the microscope.

Soft X-ray Photoelectron Spectroscopy (XPS) is one of the most important techniques for the study of the elemental ratios in the surface region. The surface sensitivity (typically 40–100 Å) makes this technique ideal for measurements as oxidation states or biomaterials powder. In this analysis we have used a VG ESCA 3 MK II XPS installation ($E_{k\alpha}$ = 1486.7 eV). The vacuum analysis chamber pressure was $P \sim 3 \times 10^{-8}$ torr. The XPS recorded spectrum involved an energy window w = 20 eV with the resolution R = 50 eV with 256 recording channels. The XPS spectra were processed using Spectral Data Processor v 2.3 (SDP) software.

The functional groups present in the prepared powder were identified by FTIR spectroscopy (Bruker Vertex 70 spectrophotometer). For this 1% of the powder was mixed and ground with 99% KBr. Tablets of 10 mm diameter for FTIR measurements were prepared by pressing the powder mixture at a load of 5 tons for 2 min and the spectrum was taken in the range of 400 to 4000 cm^{-1} with resolution 4 and 100 times scanning.

Raman studies have been carried out at the wavelength excitation of 1064 nm using a FT Raman Bruker RFS 100 spectrophotometer. The laser was operated at 100 mW power and up to 100 scans at 4 cm^{-1} resolution were accumulated.

Osteoblast MG 63 cell line (American Type Culture Collection, VA, USa0 was used in this study. Cells were seeded onto Eu:Hap discks at a density of $3x10^4$per well in 12 plates. Incubations was performed in Dulbecco's modified Eadle's medium (DMEM, Gibco, Grand Island, NY) containing 10% fetal bovine serum (FBS, Gibco), 100 µg/ml streptomycin and 100 U/ml of penicillin. The cultures were maintained in a humidified atmosphere with 5% CO_2 at 37 ^{0}C. Parallel experiments on the sterile transparent cover glasses were also performed as controls.

The evaluate cell proliferation rate quantitatively, the MG 63 cells on Eu:Hap with different Eu concentration ($0 \leq x \leq 0.015$). Six different fields per sample were randomly chosen under a microscope, and normal cells were counted at days 1, 2 and 4 respectively.

At day 4, α – tubulin (αT) staining was performed to show cell numbers on the surface of Eu:HAp discks. Briefly , The cell were fixed in 95% cold ethanol for 20 min. After two washes with PBS, cells were stained by 0.01% αT (Santa Cruz) for 2 min at room temperature, and then observed by fluorecence microscopy (Olympus IX 7 Japan using an excitation wavelength of 495 nm and emission one of 513 nm). Because cells were washed twice with PBS before αT staining, most of apoptotic or necrotic cells were washed off, and the photografhs of αT staining show the number of normal cells.

3. Results and discussions

Figure 1 displays the TEM images of pure Hap and Eu:HAp, with the atomic ratio Eu/(Eu +Ca) = 0.5% and Eu/(Eu +Ca) = 1.5% with low resolution and HRTEM. of the synthesized powder with Eu/(Eu +Ca) = 1.5%, which confirm its crystallinity. It is found that all the samples demonstrate a uniform rod-like morphology revealing that the doping components have little influence on the surface morphology of the samples. It can be seen from the HRTEM image of Eu:HAp with atomic ratio Eu/[Eu + Ca] = 1,5 % (Figure 1D) that the crystalline phase of hydroxyapatite with well-resolved lattice fringes can be observed.

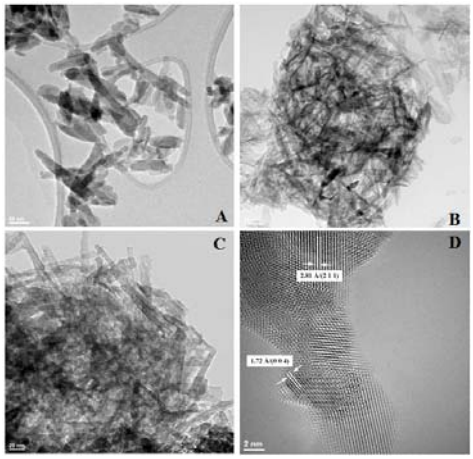

Fig. 1: TEM images of pure Hap (x = 0)(A), Eu:Hap with the atomic ratio Eu/(Eu +Ca) = 0.5% (x = 0.005)(B) and Eu/(Eu +Ca) = 1.5% (x = 0.015)(C). The HRTEM image of Eu:HAp with atomic ratio Eu/[Eu + Ca] = 1,5 % (D)

The distances (2.81 Å and 1.72 Å) between the adjacent lattice fringes agree well with the d_{211} and d_{004} spacing of the literature values (0.281 nm and 0.172 nm) (CJPDS no. 09-0432). The HRTEM images of the sample further confirm that the synthesized samples are well crystallized single crystals.

XPS technique has been tested as a useful tool for qualitatively determining the surface components and composition of the samples. **Figure 2** shows the survey XPS narrow scan spectra of Eu:HAp (x = 0.005 and x = 0.015) nanopowder. In the XPS spectrum of Eu:HAp, the binding energy of Ca (2p, 347.3 eV), O (1s, 532.1 eV), and P (2p, 133.09 eV) can be obviously found (**Figure 2**). The peaks of Eu^{3+} (3d, 1132.8 eV) agree well with the literature [28]. XPS results provide the additional evidence for the successful doping of Eu^{3+}, in Eu:HAp.

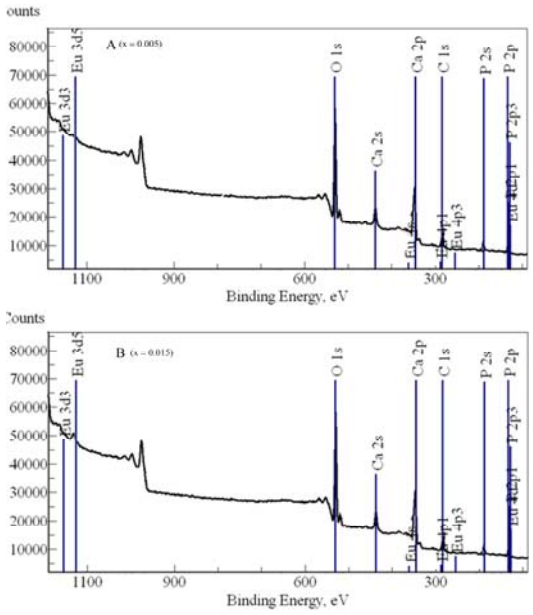

Fig. 2: The XPS survey spectrum of Eu:HAp samples synthesized with Eu/(Ca+Eu) = 0.5 % (x = 0.005), and 1.5% (x = 0.015).

Figure 3 shows the FT-IR results obtained from Eu:HAp, with the atomic ratio Eu/(Eu +Ca) =0.5% and Eu/(Eu +Ca) =1.5%. Bands at 3570 and 632 cm^{-1} are assigned to stretching mode (υ_s) and librational mode (υ_L), respectively, of the hydroxyl group, OH^-.The peak at 632 cm^{-1} is assigned to the vibration of apatitic OH^- ions. The bands at 3420 and 1641 cm^{-1} (H–O–H bond bending) showed the presence of surface water molecules [29-30]. Bands at 1091, 1033, 962, 603, 564 and 474 $cm^{-1}$are assigned to vibrations of the phosphate group, PO_4^{3-} [31-32]. The first peak at 1091 cm^{-1} emanates from a triply degenerated asymmetric stretching mode vibration, υ_3. The other component of this triply degenerated vibration, υ_3, of the P−O bond of the phosphate group appear at 1033 cm^{-1}. The peak at 962 cm^{-1} is assigned to a non-degenerated symmetric stretching mode, υ_1, of the P−O bond of the phosphate group, PO_4^{3-}. The peaks at 603 and 564 cm^{-1} are assigned to a triply degenerated bending mode, υ_4, of the O−P−O bond. The weak peak at 474 cm^{-1} is component of the doubly degenerated bending mode, υ_2, of the phosphate group. Band at 875 cm^{-1} is the characteristic peak of hydrogen phosphate group (HPO_4^{2-}).

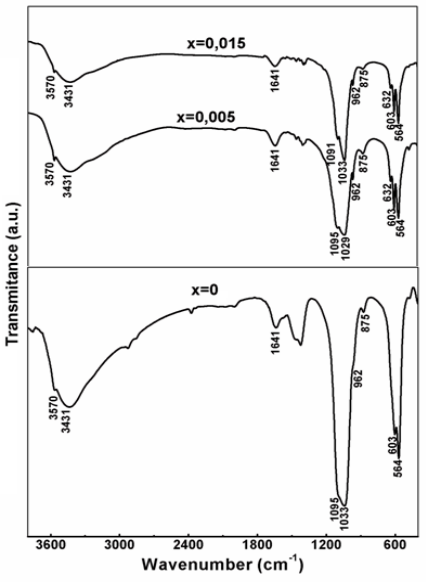

Fig. 3: FT-IR spectra of Eu:HAp with Eu/(Eu +Ca) =0.5% and Eu/(Eu +Ca) =1.5%.

The FT-Raman spectra of Eu:HAp with Eu/(Eu +Ca)=0.5% and with Eu/(Eu +Ca)=1.5% are presented in **Figure 4**. The internal modes of the PO_4^{3-} tetrahedral ν_1 frequency (960 cm^{-1}) corresponds to the symmetric stretching of P-O bonds [33]. All the samples present the very intense band at 963 cm^{-1}.

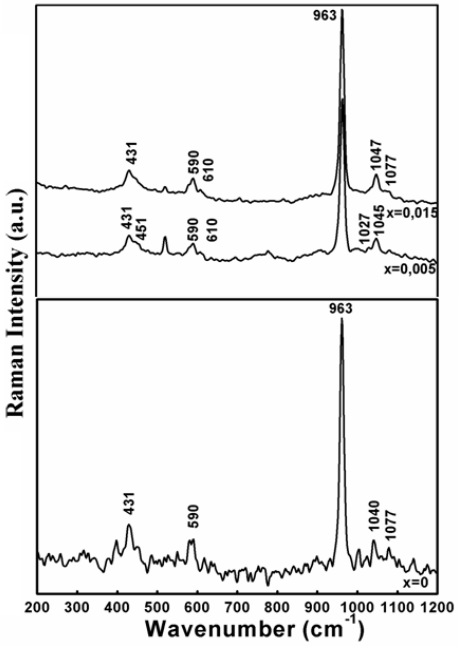

Fig. 4: FT-Raman spectra of Eu:HAp with Eu/(Eu +Ca) =0.5% and Eu:HAp with Eu/(Eu +Ca) =1.5%.

We can see that this peak at is more intense for the sample HAp Eu 1.5%. For the sample HAp Eu 0.5% were observed bands at 431 cm^{-1} and 451 cm^{-1} attributed to $\nu_2\ PO_4^{3-}$, 590 cm^{-1} and 610 cm^{-1}attributed to $\nu_4\ PO_4^{3-}$ and 1027 cm^{-1} and 1045 cm^{-1}, respectively, attributed to $\nu_3\ PO_4^{3-}$.

For the sample HAp Eu 1.5% the observed bands are shifted to: 440 cm^{-1} for $\nu_2 PO_4^{3-}$, 600 and 577 cm^{-1} for to $\nu_4 PO_4^{3-}$ and for ν_3 vibration of PO_4^{3-} at 1045 and 1077 cm^{-1}. However, the intensity of vibration peak decreases when the atomic ratio Eu/(Ca+Eu) increases.

As shown in **Figure 5** the osteoblasts MG-63 cells on pure HAp (x = 0) and Eu:HAp samples synthesized with atomic ratio Eu/(Ca+Eu) = 0.5 % (x = 0.005), and 1.5% (x = 0.015) proliferated with increasing culturing time (up to 4 days).

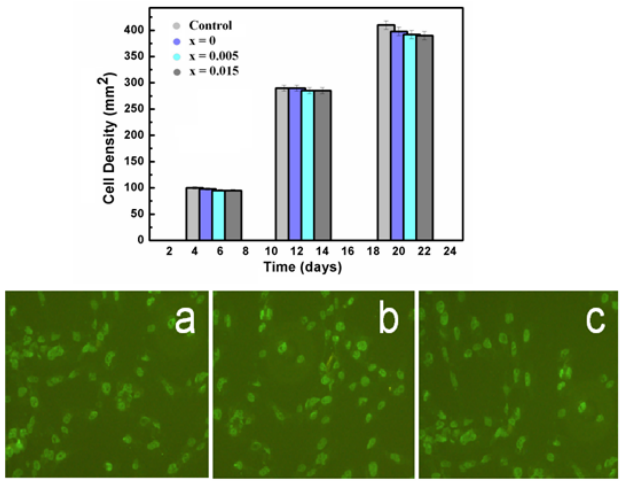

Fig. 5: Cell density of MG-63 on different samples for 1, 2 and 4 days (top); Fluorescence microscopic photographs of MG-63 cells (cultured for 4 days) on HAp (x = 0) and Eu:HAp with Eu/(Eu +Ca) =0.5% (x = 0.005) and Eu:HAp with Eu/(Eu +Ca) =1.5 (x = 0.015) (bottom).

Furthermore, cell number was significantly higher after 4 days of incubation, though there was no significant difference between both surfaces after 1 and 2 days of incubation. None of the ceramics modified the cellular morphology in term of size and shape is observed. The number of osteoblasts MG-63 cells on control, pure HAp (x = 0) and and Eu:HAp samples synthesized with atomic ratio Eu/(Ca+Eu) = 0.5 % (x = 0.005), and 1.5% (x = 0.015) was 410±25, 398±20, 392±21, 390±16 after 4 days.

4. Conclusions

In this study, the Eu concentration controlled nano-Hap particles were synthesized and their Eu concentration on osteoblast cells was evaluated. Our results demonstrate that cell proliferation is not related to the Eu concentration in the samples. All the samples exhibits the characteristic bands attributed to the PO_4^{3-} vibrations. Results obtained by FT Raman spectroscopy are in good agreement with results obtained by FTIR spectroscopy. XPS results provide the additional evidence for the successful doping of Ag^{+}, in Ag:HAp. This work provides an interesting view of the role of europium doped HAp nanoparticles as ideal biomaterials in future clinical applications.

Acknowledgements

The authors would like to acknowledge Dr. Philippe Le Coustumer for his constructive discussions for the Transmission Electron Microscopy analysis. The authors wish to thank Alina Mihaela Prodan for assistance with biological test.

References

[1] W.F. De Jong, J. Bouman, J.J. De Lange, Physica, **5(3)**, 188 (1938).
[2] C. P.A.T. Klein, Y. Abe, H. Hosono, K. de Groot, Biomaterials, **8(3)**, 234 (1987).
[3] W. Bonfield, J. of Biomedical Engineering, **10(6)**, 522 (1988).
[4] M. Vallet-Regi, J. M. González-Calbet, Prog. Solid State Sci., **32**, 1 (2004).
[5] S. Weiner, L. Addadi, J. Mater. Chem., **7**, 689 (1997).
[6] M. Elisa, C. Grigorescu, I. Vasiliu, M. Bulinski, V. Kuncser, D. Predoi, G. Filoti, A. Meghea, N. Iftimie, M. Giurginca and C. Onose, Opt. Quant. Electron., **4(6)**, 523 (2007).
[7] A. Costescu, I. Pasuk, F. Ungureanu, A. Dinischiotu, M. Costache, F. Huneau, S. Galaup, P.Le. Coustumer, D. Predoi, Dig. J.Nanomater Bios., **5(4)**, 989 (2010).
[8] D. M. Liu, T. Troczynski, W. J. Tseng, Biomaterials, **23(4)**, 1227 (2002).
[9]D. Predoi and R.A. Vatasescu-Balcan, J. Optoelectron. Adv. M., **10(1)**, 152, (2008).
[10] D. Predoi, R.A. Vatasescu-Balcan, I. Pasuk, R. Trusca and M. Costache, J. Optoelectron. Adv. Mater., **10(8)**, 2151 (2008).
[11]. C.E. Secu, D. Predoi, M.Secu, M. Cernea, G. Aldica, Opt. Mater., **31**(11), 1745 (2009).
[12] S. Weiner, H.D. Wagner, Annual, Rev. of Mat., Sci. **28**, 271 (1998).
[13] T. J. Issacs, J. Electrochem. Soc., **120**, 654 (1973).
[14] C. Feldmann, T. Justel, C.R. Ronda, P.J. Schmidt, Adv. Funct. Mater., **13(7)**, 511 (2003).
[15] C.S. Ciobanu, E. Andronescu, A. Stoicu, O. Florea, P.Le Coustumer, S. Galaup, A. Adjouadi, J.Y. Mevellec, I. Musa, F. Massuyeau, A. M. Prodan, K. Lafdi, R. Trusca, I. Pasuk, D. Predoi, Dig. J. Nanomater. Bios. **6 (2)**, 609 (2011).
[16] F. Ungureanu, D. Predoi, R.V. Ghita, R.A. Vatasescu-Balcan, M. Costache, Interface Controled Organic Thin Films, **1**, 67 (2009).
[17] L. Boyer, B. Piriou, J. Carpena, J.L. Lacout, J. Alloys Compd., **311**, 143 (2000).
[18] S. Ekambaram, K. C. Patil, M. Maaza, J.Alloys Compd., **393**, 81 (2005).
[19] P. Sibilla, A. Sereni, G. Aguiari, M. Banzi, E. Manzati, C. Mischiati, J. Dent. Res., **85**, 354 (2006).
[20] S. Dasgupta, A. Bandyopadhyay, S. Bose, Acta Biomater., **5(8)**, 3112 (2009).
[21] T.Y. Liu, S.Y. Chen, D.M. Liu, S.C. Liou, J. Control. Release, **107**, 112 (2005).
[22] B. Palazzo, M. Iafisco, M. Laforgia, N. Margiotta, G. Natile, C.L. Bianchi, Adv. Funct. Mater., **17**, 2180 (2007).
[23] X. Zhu, O. Eibl, L. Scheideler, J. Geis-Gerstorfer, J. Biomed. Mater. Res. A, **79A**, 114 (2006).
[24] X. Zhu, O. Eibl, C. Berthold, L. Scheideler, J.Geis-Gerstorfer, Nanotechnology, **17**, 2711 (2006).
[25] Y. R. Cai, Y. K. Liu, W. Q. Yan, Q. H. Hu , J. H. Tao, M. Zhang, Z. L. Shi , R. K. Tang, J. Mater. Chem. **17**, 3780 (2007).
[26] W. Andreoni, D. Scharf, P. Giannozzi, Chem. Phys. Lett., **173(5-6),** 449 (1990).
[27] C. S. Ciobanu, E. Andronescu, B.S. Vasile, C.M. Valsangiacom, R.V. Ghita, D. Predoi, Optoelectron. Adv. Mater. – Rapid Comm., **4(10)**, 1515 (2010).
[28] D. Predoi, S. Derible, H. Duflo, J. Optoelectron. Adv. Mat., **4(1)**, 110, (2010).
[29] C. Birsan, D. Predoi and E. Andronescu, J. Optoelectron. Adv. Mat., **9(6)**, 1821-1824 (2007).
[30] M. Birsan, D. Predoi, C. Birsan, C.E. Secu and E. Andronescu, J. Optoelectron. Adv. Mater., **9(6)**, 1829 (2007).
[31] D. Predoi, R.V. Ghita, F. Ungureanu, C.C. Negrila, R.A. Vatasescu-Balcan and M.Costache, J. Optoelectron. Adv. Mater., **9(12)**, 3827 (2007).
[32] D. Predoi, M. Barsan, E. Andronescu, R.A. Vatasescu-Balcan and M. Costache, J. Optoelectron. Adv. Mater. **9(11)**, 3609 (2007).
[33] C.S. Ciobanu, F. Massuyeau, E. Andronescu, M.S. Stan, A. Dinischiotu, D. Predoi, Dig. J. Nanomater. Bios. **6(4)**, 1639 (2011).